

Magnetic fields in galaxy clusters

Christoph Pfrommer

Heidelberg Institute for Theoretical Studies, Germany

Jul 30, 2014 / *Inhomogeneities in the Intracluster Plasma*,
Stanford



Outline

- 1 Intracluster magnetic fields
 - Origin and evolution
 - Faraday rotation measures
 - Minimum field estimates
- 2 Fields at cluster shocks
 - Radio relics
 - Radio and X-rays
 - Cooling lengths
- 3 Magnetic draping
 - Mechanism
 - Observations
 - MHD Simulations



Outline

- 1 **Intracluster magnetic fields**
 - Origin and evolution
 - Faraday rotation measures
 - Minimum field estimates
- 2 Fields at cluster shocks
 - Radio relics
 - Radio and X-rays
 - Cooling lengths
- 3 Magnetic draping
 - Mechanism
 - Observations
 - MHD Simulations



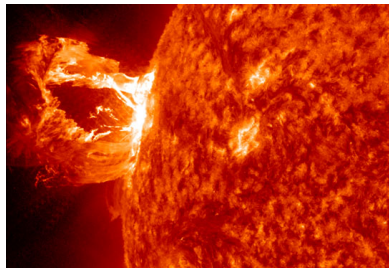
Origin and evolution of cluster fields

possible origin:

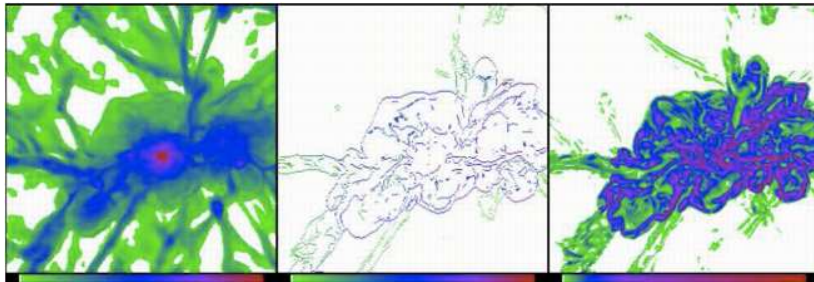
- **stellar winds or AGN jets**
- **plasma instabilities or battery effects** in shock waves, in ionization fronts, or in neutral gas-plasma interactions
- **primordial generation in early universe processes**, such as phase transitions during the epoch of inflation

evolution:

- amplification in a (small-scale turbulent) dynamo
- expectation: saturation at a fraction of P_{kin}



Origin of turbulence and magnetic fields



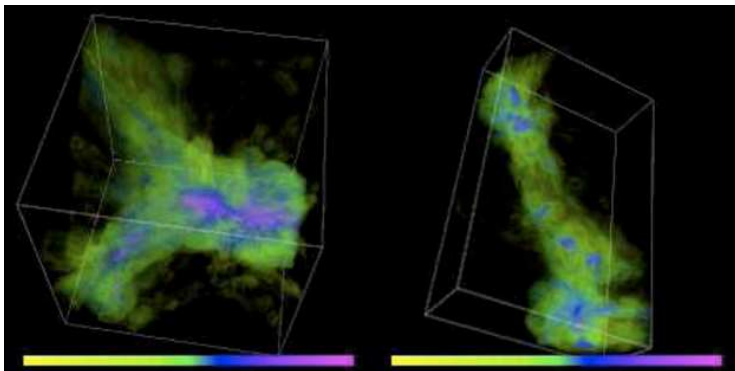
gas density, locations of shocks, vorticity = curl of flow velocity (Ryu et al. 2008)

model for the origin of intra-cluster magnetic fields:

- turbulent flow motions are induced via the cascade of the vorticity generated at cosmological formation shocks
- the turbulence amplifies weak seed magnetic fields of any origin



Volume rendered magnetic field strengths



distribution of the resulting inter-galactic magnetic fields around a cluster and a filament that includes a number of groups (Ryu et al. 2008)

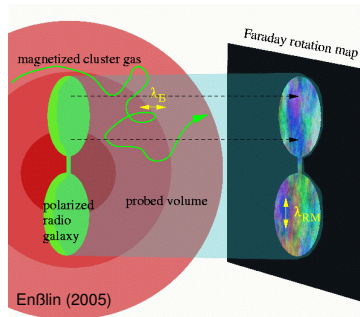
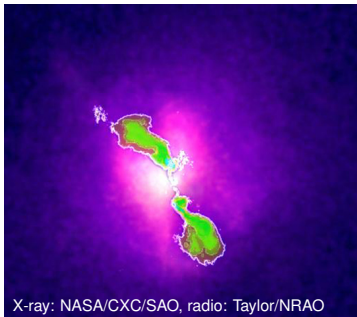


Faraday rotation measurements

magnetic birefringence causes rotation of plane of polarization

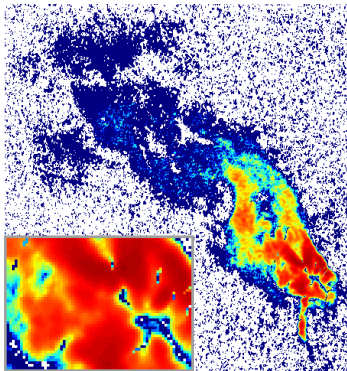
$$\chi(\mathbf{x}_\perp, \lambda) = \chi_0 + \lambda^2 \frac{e^3}{2\pi m_e^2 c^4} \int_0^{z_s} dz n_e(\mathbf{x}_\perp, z) B_z(\mathbf{x}_\perp, z)$$

- need to model n_e and window function \rightarrow statistics of $B_z(\mathbf{x}_\perp)$
- assuming statistical isotropy \rightarrow deprojection and statistics of B

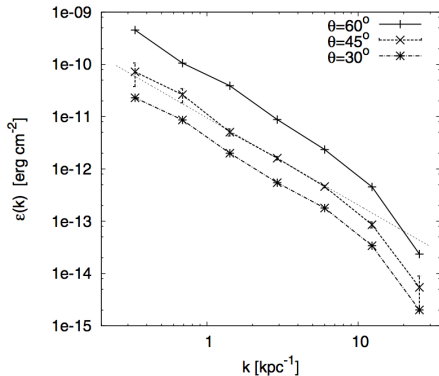


Faraday rotation measurements: Hydra A

- inferred power spectrum compatible with Kolmogorov slope
- $B_0 = 36 \mu\text{G}$ (45°) and coherence scale $> 8 \text{ kpc}$



Vogt+ (2005)



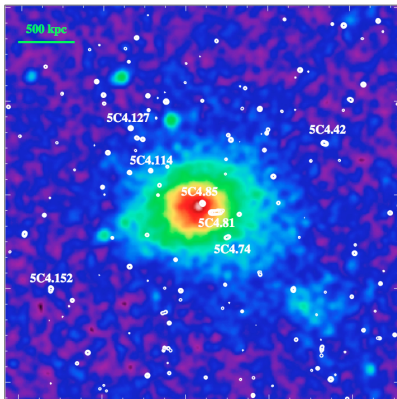
Kuchar & Enßlin (2011)



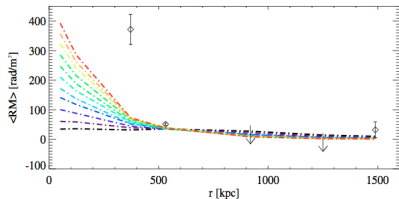
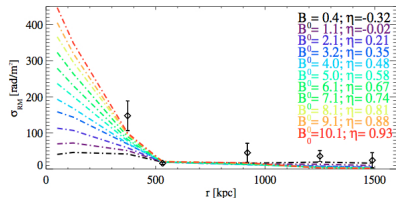
HITS

Faraday rotation measurements: Coma

- forward modeling of 3D magnetic (Kolmogorov) power spectra
- varying B_0 and radial magnetic decline ($B \propto n_e^\eta$): $B_0 \simeq 5 \mu\text{G}$, $\eta \simeq 0.5$

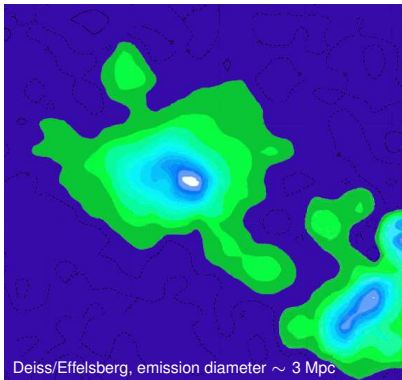


Bonafede+ (2010)

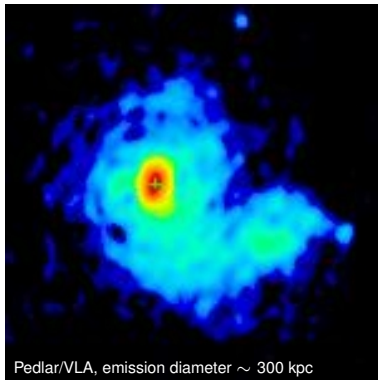


Radio (mini-)halos: Coma and Perseus

Coma radio halo:



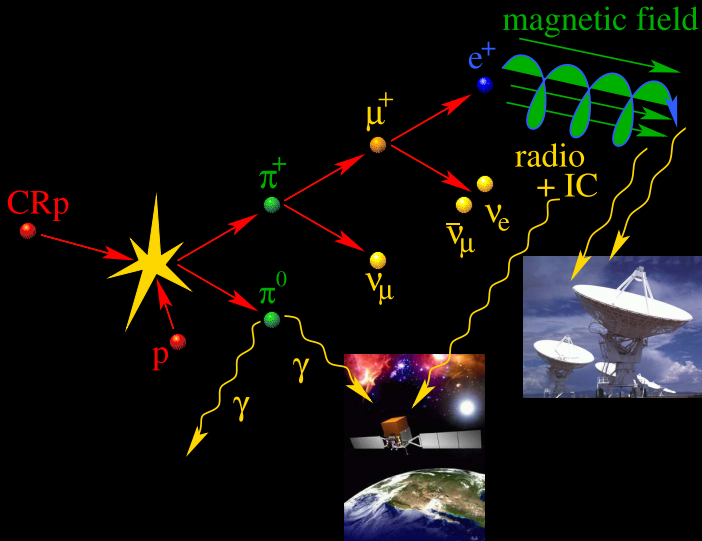
Perseus mini-halo:



emission models: **turbulent re-acceleration** or **hadronic cosmic ray interactions?**

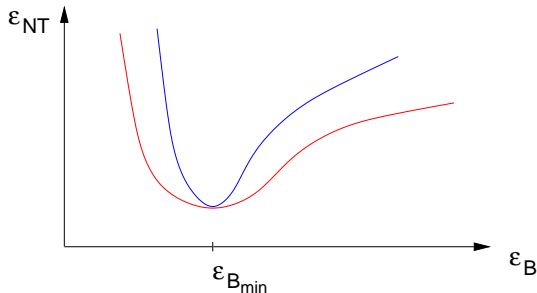


Hadronic cosmic ray proton interaction



Minimum energy criterion (MEC): the idea

- $\varepsilon_{\text{NT}} = \varepsilon_B + \varepsilon_{\text{CRp}} + \varepsilon_{\text{CRe}}$
 → minimum energy criterion: $\left. \frac{\partial \varepsilon_{\text{NT}}}{\partial \varepsilon_B} \right|_{j_\nu} \stackrel{!}{=} 0$
- classical MEC: $\varepsilon_{\text{CRp}} = k_p \varepsilon_{\text{CRe}}$
- hadronic MEC: $\varepsilon_{\text{CRp}} \propto (\varepsilon_B + \varepsilon_{\text{CMB}}) \varepsilon_{\text{CRe}} \propto (\varepsilon_B + \varepsilon_{\text{CMB}}) \varepsilon_B^{-(\alpha_\nu + 1)/2} j_\nu$

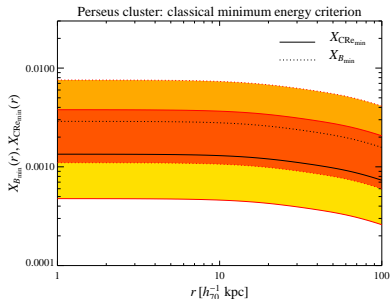
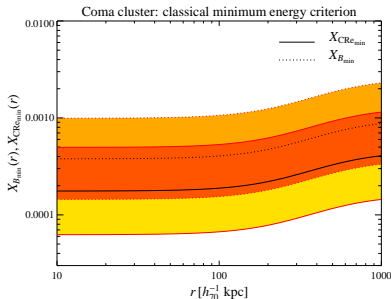


define tolerance levels:
 deviation from minimum
 by one e-fold



Classical minimum energy criterion

$$X_{\text{CRp}}(r) = \frac{\varepsilon_{\text{CRp}}}{\varepsilon_{\text{th}}}(r), \quad X_B(r) = \frac{\varepsilon_B}{\varepsilon_{\text{th}}}(r)$$



C.P. & Enßlin (2004)

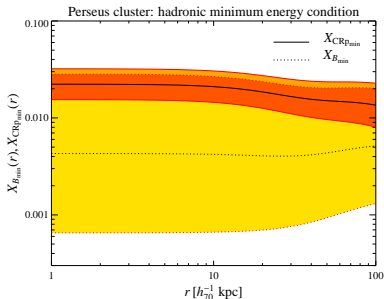
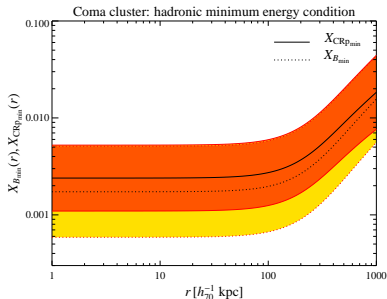
$$B_{\text{Coma}}(0) = 1.1^{+0.7}_{-0.4} \mu\text{G}$$

$$B_{\text{Perseus}}(0) = 7.2^{+4.5}_{-2.8} \mu\text{G}$$



Hadronic minimum energy criterion

$$X_{\text{CRp}}(r) = \frac{\varepsilon_{\text{CRp}}}{\varepsilon_{\text{th}}}(r), \quad X_B(r) = \frac{\varepsilon_B}{\varepsilon_{\text{th}}}(r)$$



C.P. & Enßlin (2004)

$$B_{\text{Coma}}(0) = 2.4^{+1.7}_{-1.0} \mu\text{G}$$

$$B_{\text{Perseus}}(0) = 8.8^{+13.8}_{-5.4} \mu\text{G}$$

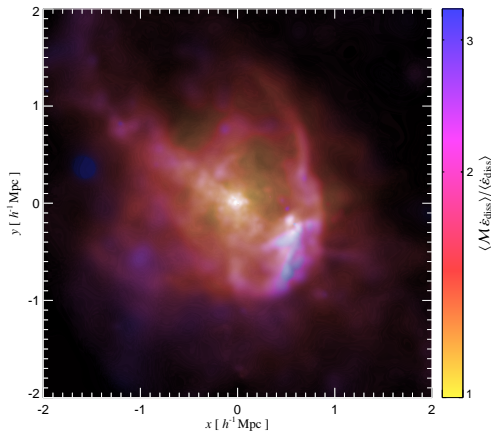


Outline

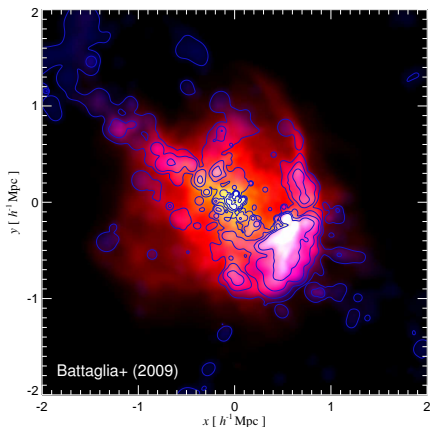
- 1 Intracluster magnetic fields
 - Origin and evolution
 - Faraday rotation measures
 - Minimum field estimates
- 2 **Fields at cluster shocks**
 - Radio relics
 - Radio and X-rays
 - Cooling lengths
- 3 Magnetic draping
 - Mechanism
 - Observations
 - MHD Simulations



Radio gischt illuminates cluster magnetic fields



structure formation shocks triggered by a recent merger of a large galaxy cluster.



red/yellow: shock-dissipated energy,
blue/contours: 150 MHz radio gischt emission from shock-accelerated CRe



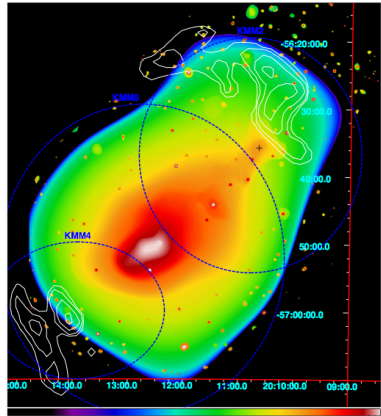
Synchrotron and inverse Compton emission

detection of hard X-ray emission at the northern relic of A3667:

$$\frac{F_{\text{sync}}}{F_{\text{IC}}} \propto \frac{\epsilon_B^{(\alpha_e+1)/4}}{\epsilon_{\text{CMB}}} \left(\frac{\nu_{\text{sync}}}{\nu_{\text{IC}}} \right)^{(1-\alpha_e)/2}$$

- if X-ray emission due to thermal bremsstrahlung: lower B limit
- if X-ray emission due to inverse Compton: estimate for B provided the radio emitting regions correlate with the volume occupied by B

→ $B > 3\mu\text{G}$ at the relic, i.e. at R_{200} !

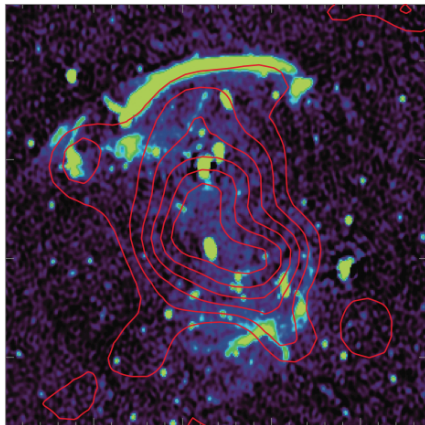


Finoguenov+ (2010)



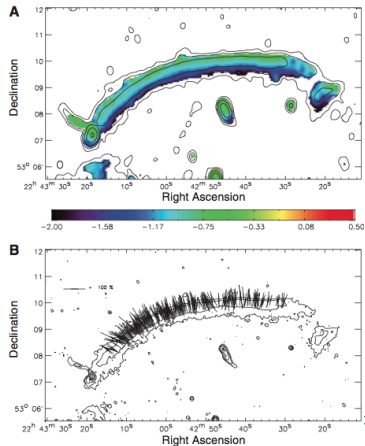
Radio gischt probes acceleration and magnetic fields

double relic in CIZA J2242:



van Weeren+ (2010)

spectral index + E polarization:

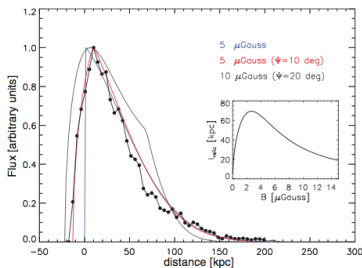
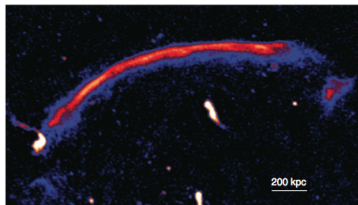


Radio gischt probes acceleration and magnetic fields

- synchrotron cooling length of equilibrium electron distribution:

$$l_{\text{sync}} = v_{\text{adv}} \tau_{\text{sync}} \propto \frac{\sqrt{B}}{B^2 + B_{\text{CMB}}^2}$$

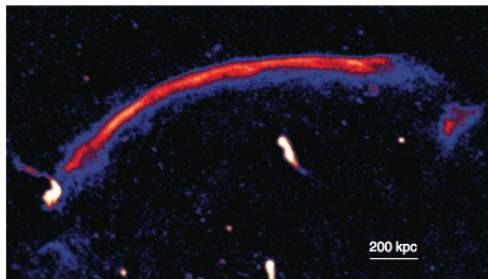
- allows for 2 solutions:
 $B \geq 5 \mu\text{G}$ or $B \leq 1.2 \mu\text{G}$
 accounting for projection effects
- van Weeren+ argue for $B \geq 5 \mu\text{G}$
 solution based X-ray limits in
 A3667



van Weeren+ (2010)

HITS

Radio gischt probes acceleration and magnetic fields



van Weeren+ (2010)

- how are these strong magnetic fields at the center out to R_{200} generated?
- why is the magnetic field perpendicular to the shock normal?
- how can particle acceleration proceed at perpendicular shocks?

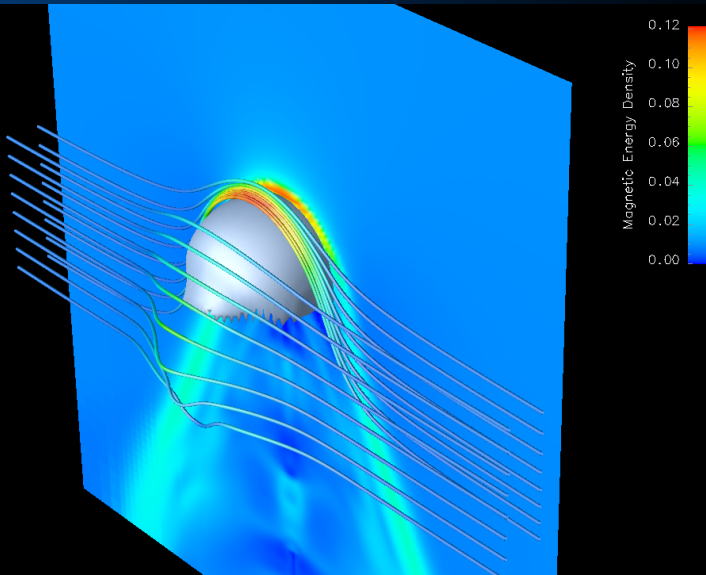


Outline

- 1 Intracluster magnetic fields
 - Origin and evolution
 - Faraday rotation measures
 - Minimum field estimates
- 2 Fields at cluster shocks
 - Radio relics
 - Radio and X-rays
 - Cooling lengths
- 3 **Magnetic draping**
 - Mechanism
 - Observations
 - MHD Simulations

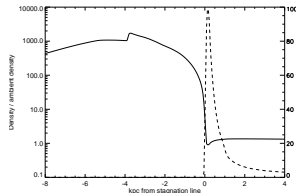


What is magnetic draping?



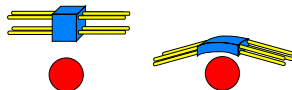
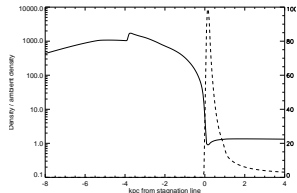
What is magnetic draping?

- is magnetic draping (MD) similar to ram pressure compression?
 - no density enhancement for MD
 - analytical solution of MD for incompressible flow
 - ideal MHD simulations (*right*)



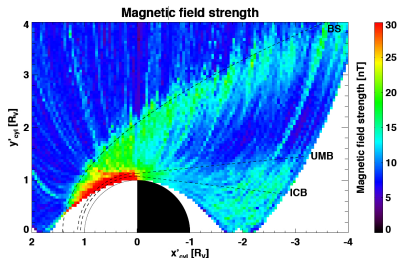
What is magnetic draping?

- is magnetic draping (MD) similar to ram pressure compression?
→ no density enhancement for MD
 - analytical solution of MD for incompressible flow
 - ideal MHD simulations (*right*)
- is magnetic flux still frozen into the plasma?
yes, but plasma is pulled into the direction of the field lines while field lines get stuck at the obstacle



Draping of the interplanetary field over Venus

- Venus and Mars do not have a global magnetic field
- *Venus Express*: amplification of solar wind field by a factor ~ 6 at the side facing the Sun

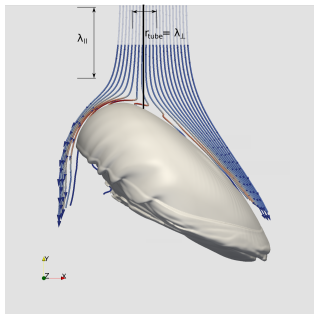


Guicking et al. (2010)

- draping of solar wind magnetic field around Venus/Mars leads to the **formation of magnetic pile-up region and the magneto tail**
→ enhanced magnetic field strength in the planets' wake



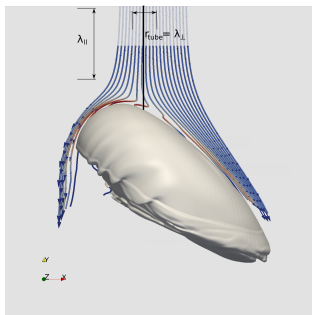
Streamlines in the rest frame of the galaxy



- Stokes function $p(s, \theta) = \sqrt{3sR} \sin \theta$
 → critical impact parameter for $\theta = \pi/2$, $s = l_{\text{drape}}$: $p_{\text{cr}} = R/(2\mathcal{M}_A)$
- only those streamlines initially in a narrow tube of radius $p_{\text{cr}} \simeq R/20 \simeq 1 \text{ kpc}$ from the stagnation line become part of the magnetic draping layer (color coded)
 → constraints on λ_B



Streamlines in the rest frame of the galaxy



- Stokes function $p(s, \theta) = \sqrt{3sR} \sin \theta$
→ critical impact parameter for $\theta = \pi/2$, $s = l_{\text{drape}}$: $p_{\text{cr}} = R/(2\mathcal{M}_A)$
- only those streamlines initially in a narrow tube of radius $p_{\text{cr}} \simeq R/20 \simeq 1 \text{ kpc}$ from the stagnation line become part of the magnetic draping layer (color coded)
→ constraints on λ_B
- the streamlines that do not intersect the tube get deflected away from the galaxy, become never part of the drape and eventually get accelerated (Bernoulli effect)
- note the kink feature in some draping-layer field lines due to back reaction as the solution changes from the hydrodynamic potential flow solution to that in the draped layer



Conditions for magnetic draping

- **ambient plasma sufficiently ionized** such that flux freezing condition applies
- **super-Alfvénic motion** of a cloud through a weakly magnetized plasma: $\mathcal{M}_A^2 = \beta\gamma\mathcal{M}^2/2 > 1$
- **magnetic coherence across the “cylinder of influence”:**

$$\frac{\lambda_B}{R} \gtrsim \frac{1}{\mathcal{M}_A} \sim 0.1 \times \left(\frac{\beta}{100} \right)^{-1/2} \quad \text{for sonic motions,}$$

Here R denotes the curvature radius of the working surface at the stagnation line.



Polarized synchrotron emission in a field spiral: M51

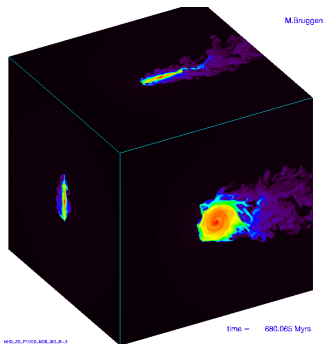


MPIfR Bonn and Hubble Heritage Team

- grand design 'whirlpool galaxy' (M51): optical star light superposed on radio contours
- polarized radio intensity follows the spiral pattern and is strongest in between the spiral arms
- the polarization 'B-vectors' are aligned with the spiral structure



Ram-pressure stripping of cluster spirals



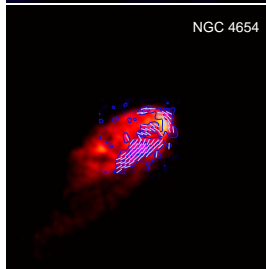
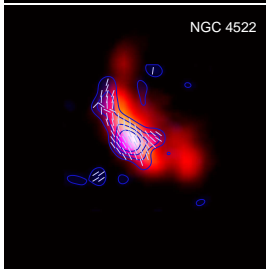
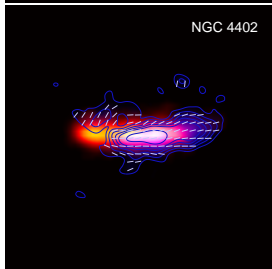
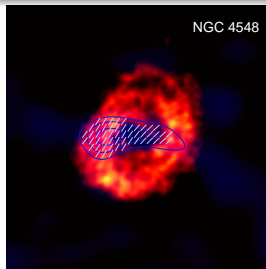
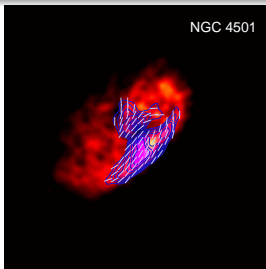
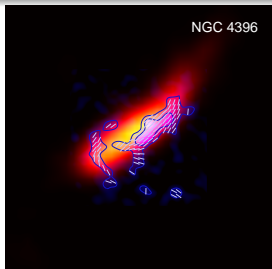
Brueggen (2008)

- 3D simulations show that the ram-pressure wind quickly strips the low-density gas in between spiral arms (Tonnesen & Bryan 2010)
- being flux-frozen into this dilute plasma, the large scale magnetic field will also be stripped

→ resulting radio emission should be unpolarized



Polarized synchrotron ridges in Virgo spirals



Vollmer et al. (2007): 6 cm PI (contours) + B-vectors; Chung et al. (2009): HI (red)



Observational evidence and model challenges

- asymmetric distributions of polarized intensity at the leading edge with extraplanar emission, sometimes also at the side
- coherent alignment of polarization vectors over ~ 30 kpc
- HI gas only moderately enhanced (factor $\lesssim 2$), localized 'HI hot spot' smaller than the polarized emission region:

$$n_{\text{compr}} \simeq n_{\text{icm}} v_{\text{gal}}^2 / c_{\text{ism}}^2 \simeq 1 \text{ cm}^{-3} \simeq \langle n_{\text{ism}} \rangle$$



Observational evidence and model challenges

- asymmetric distributions of polarized intensity at the leading edge with extraplanar emission, sometimes also at the side
- coherent alignment of polarization vectors over ~ 30 kpc
- HI gas only moderately enhanced (factor $\lesssim 2$), localized ‘HI hot spot’ smaller than the polarized emission region:
$$n_{\text{compr}} \simeq n_{\text{icm}} v_{\text{gal}}^2 / c_{\text{ism}}^2 \simeq 1 \text{ cm}^{-3} \simeq \langle n_{\text{ism}} \rangle$$
- stars lead polarized emission, polarized emission leads gas
- flat radio spectral index (similar to the Milky Way) that steepens towards the edges of the polarized ridge
- no or weak Kelvin-Helmholtz instabilities at interface detectable



Observational evidence and model challenges

- asymmetric distributions of polarized intensity at the leading edge with extraplanar emission, sometimes also at the side
- coherent alignment of polarization vectors over ~ 30 kpc
- HI gas only moderately enhanced (factor $\lesssim 2$), localized ‘HI hot spot’ smaller than the polarized emission region:

$$n_{\text{compr}} \simeq n_{\text{icm}} v_{\text{gal}}^2 / c_{\text{ism}}^2 \simeq 1 \text{ cm}^{-3} \simeq \langle n_{\text{ism}} \rangle$$
- stars lead polarized emission, polarized emission leads gas
- flat radio spectral index (similar to the Milky Way) that steepens towards the edges of the polarized ridge
- no or weak Kelvin-Helmholtz instabilities at interface detectable

→ previous models that use ram-pressure compressed galactic magnetic fields fail to explain most of these points!



Observational evidence and model challenges

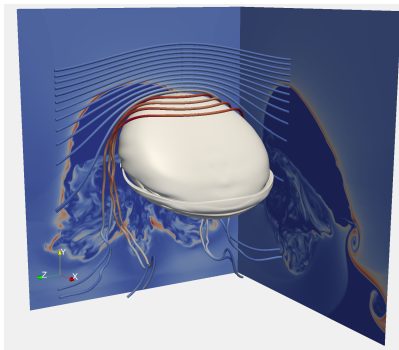
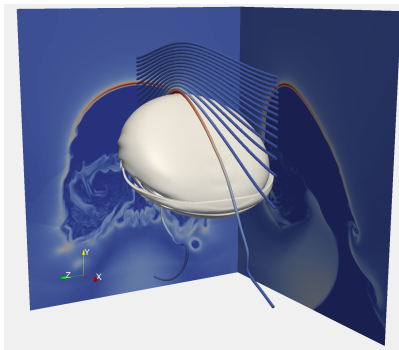
- asymmetric distributions of polarized intensity at the leading edge with extraplanar emission, sometimes also at the side
- coherent alignment of polarization vectors over ~ 30 kpc
- HI gas only moderately enhanced (factor $\lesssim 2$), localized ‘HI hot spot’ smaller than the polarized emission region:

$$n_{\text{compr}} \simeq n_{\text{icm}} v_{\text{gal}}^2 / c_{\text{ism}}^2 \simeq 1 \text{ cm}^{-3} \simeq \langle n_{\text{ism}} \rangle$$
- stars lead polarized emission, polarized emission leads gas
- flat radio spectral index (similar to the Milky Way) that steepens towards the edges of the polarized ridge
- no or weak Kelvin-Helmholtz instabilities at interface detectable

→ need to consider the full MHD of the interaction spiral galaxy and magnetized ICM !



Magnetic draping around a spiral galaxy

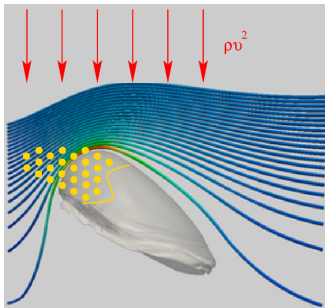


Athena simulations of spiral galaxies interacting with a uniform cluster magnetic field. There is a **sheath of strong field draped around the leading edge (shown in red)**.

C.P. & Dursi, 2010, Nature Phys.



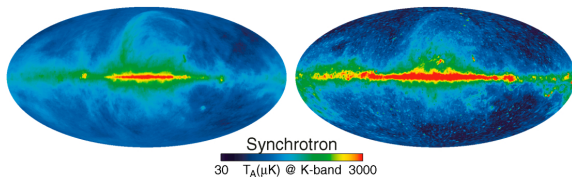
Magnetic draping around a spiral galaxy – physics



- the galactic ISM is pushed back by the ram pressure wind $\sim \rho v^2$
 - the stars are largely unaffected and lead the gas
 - the draping sheath is formed at the contact of galaxy/cluster wind
 - as stars become SN, their remnants accelerate CRes that populate the field lines in the draping layer
-
- CRes are transported diffusively (along field lines) and advectively as field lines slip over the galaxy
 - CRes emit radio synchrotron radiation in the draped region, tracing out the field lines there → **coherent polarized emission at the galaxies' leading edges**



Modeling the electron population



- typical SN rates imply a homogeneous CRe distribution (WMAP)
- FIR-radio correlation of Virgo spirals show comparable values to the solar circle → take CRe distribution of our Galaxy:

$$n_{\text{cre}} = C_0 e^{-(R-R_\odot)/h_R} e^{-|z|/h_z}$$

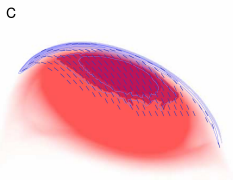
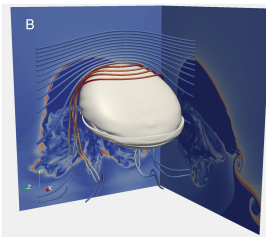
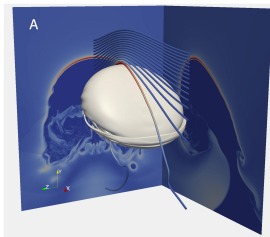
with normalization $C_0 \simeq 10^{-4} \text{ cm}^{-3}$,
scale heights $h_R \simeq 8 \text{ kpc}$ and $h_z \simeq 1 \text{ kpc}$ at Solar position

- truncate at contact of ISM-ICM, attach exp. CRe distribution \perp to contact surface with $h_\perp \simeq 150 \text{ pc}$ (max. radius of Sedov phase)

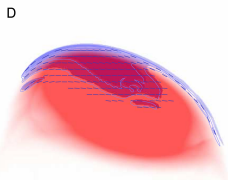


Magnetic draping and polarized synchrotron emission

Synchrotron B-vectors reflect the upstream orientation of cluster magnetic fields



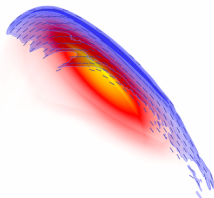
Total PI = 8.227 mJy
Max PI = 218.7 μ Jy/beam



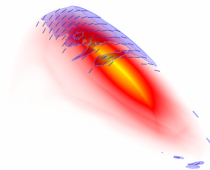
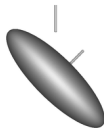
Total PI = 8.440 mJy
Max PI = 334.6 μ Jy/beam



Simulated polarized synchrotron emission



Total PI (mJ) = 23.47
Max PI (μ J/beam) = 3002.



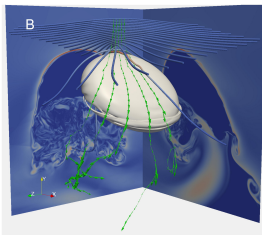
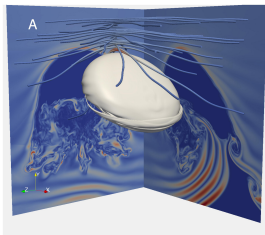
Total PI (mJ) = 4.114
Max PI (μ J/beam) = 133.9

Movie of the simulated polarized synchrotron radiation viewed from various angles and with two field orientations.

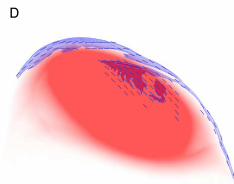


Magnetic draping of a helical B-field

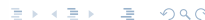
(Non-)observation of polarization twist constrains magnetic coherence length



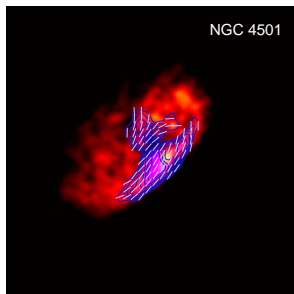
Total PI = 1.586 mJ
Max PI = 67.42 μ J/beam



Total PI = 5.927 mJ
Max PI = 304.9 μ J/beam



Magnetic coherence scale estimate by radio ridges



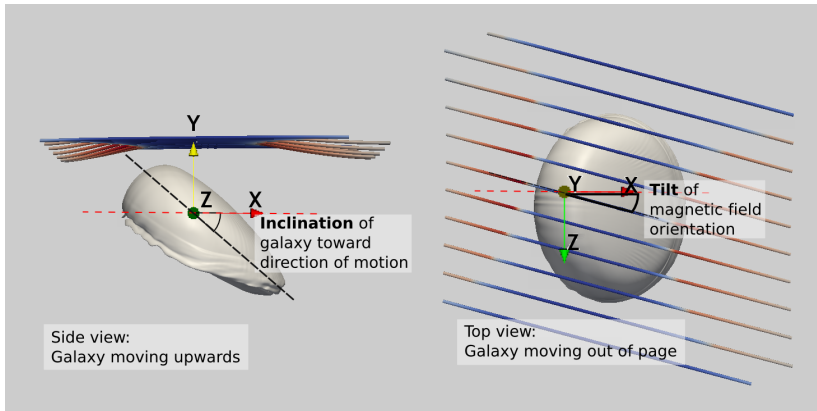
- observed polarised draping emission
 → field coherence length λ_B is at least galaxy-sized
- if $\lambda_B \sim 2R_{\text{gal}}$, then the change of orientation of field vectors imprint as a change of the polarisation vectors along the vertical direction of the ridge showing a ‘polarisation-twist’
- the reduced speed of the boundary flow means that a small L_{drape} corresponds to a larger length scale of the unperturbed magnetic field ahead of the galaxy NGC 4501

$$L_{\text{coh}} \simeq \eta L_{\text{drape}} v_{\text{gal}} / v_{\text{drape}} = \eta \tau_{\text{syn}} v_{\text{gal}} > 100 \text{ kpc},$$

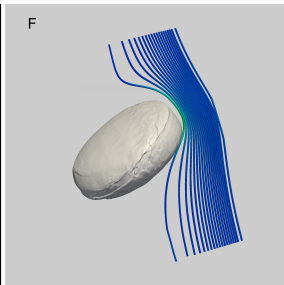
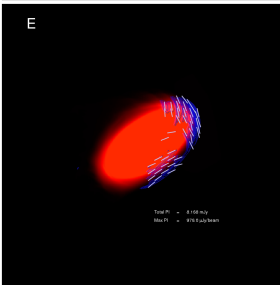
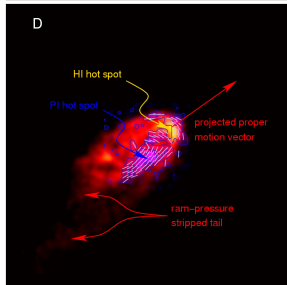
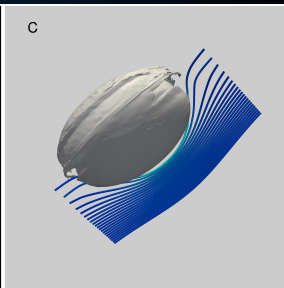
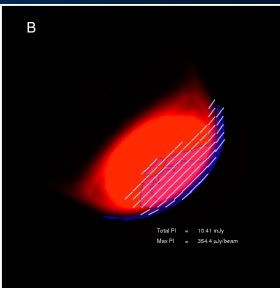
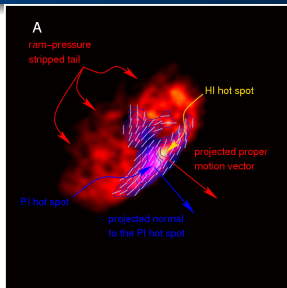
with $\tau_{\text{syn}} \simeq 5 \times 10^7 \text{ yr}$, $v_{\text{gal}} \simeq 1000 \text{ km/s}$, and a geometric factor $\eta \simeq 2$



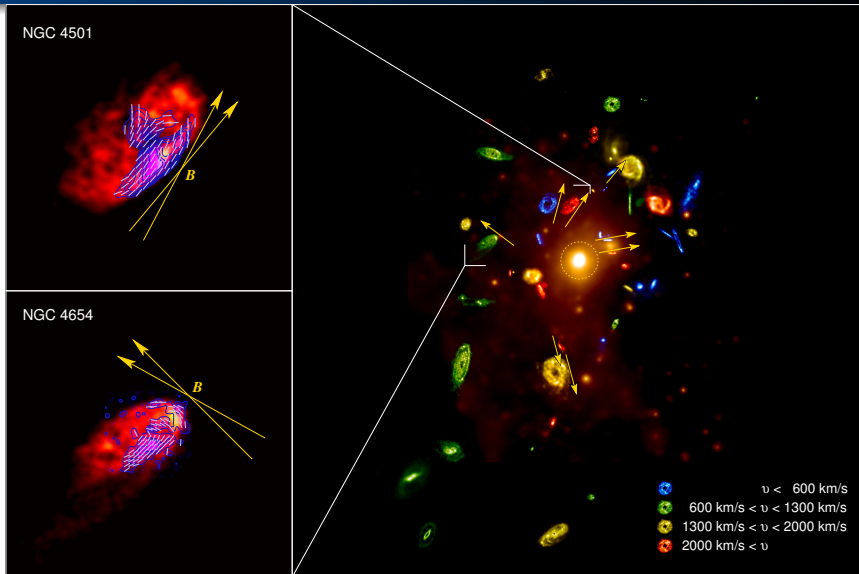
Varying galaxy inclination and magnetic tilt



Observations versus simulations



Mapping out the magnetic field in Virgo



Discussion of radial field geometry

- The alignment of the field in the plane of the sky is **significantly more radial than expected from random chance**. Considering the sum of deviations from radial alignment gives a chance coincidence of less than 1.7% ($\sim 2.2 \sigma$).
- For the **three nearby galaxy pairs** in the data set, **all have very similar field orientations**.

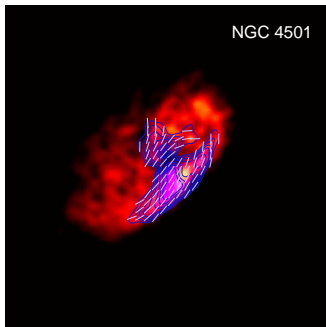
→ Which effect causes this field geometry?

Magneto-thermal instability? (Parrish+2007)

Radial infall? (Ruszkowski+2010)



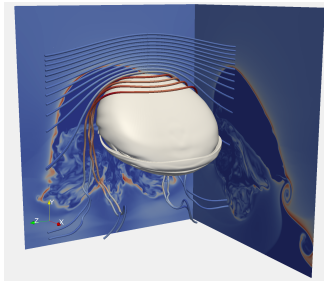
Conclusions on magnetic draping around galaxies



- draping of cluster magnetic fields naturally explains polarization ridges at Virgo spirals



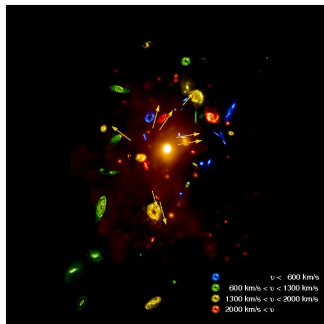
Conclusions on magnetic draping around galaxies



- draping of cluster magnetic fields naturally explains polarization ridges at Virgo spirals
- this represents a new tool for measuring the in situ 3D orientation and coherence scale of cluster magnetic fields



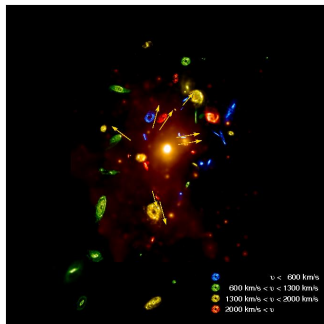
Conclusions on magnetic draping around galaxies



- draping of cluster magnetic fields naturally explains polarization ridges at Virgo spirals
- this represents a new tool for measuring the in situ 3D orientation and coherence scale of cluster magnetic fields
- application to the Virgo cluster shows that the magnetic field is preferentially aligned radially



Conclusions on magnetic draping around galaxies



- draping of cluster magnetic fields naturally explains polarization ridges at Virgo spirals
 - this represents a new tool for measuring the in situ 3D orientation and coherence scale of cluster magnetic fields
 - application to the Virgo cluster shows that the magnetic field is preferentially aligned radially
-
- this finding implies efficient thermal conduction across clusters
→ thermal cluster history & cluster cosmology
 - prospects for studying microphysics of transport processes, issues: magnetic reconnection with ISM fields



Literature for the talk

- Pfrommer & Dursi, 2010, *Nature Phys.*, 6, 5206, *Detecting the orientation of magnetic fields in galaxy clusters*
- Dursi & Pfrommer, 2008, *ApJ*, 677, 993, *Draping of cluster magnetic fields over bullets and bubbles - morphology and dynamic effects*



Additional slides



Biases in inferring the field orientation

- uncertainties in estimating the 3D velocity: v_r , ram-pressure stripped gas visible in HI morphology $\rightarrow \hat{\mathbf{v}}_t$
- *direction-of-motion asymmetry*: magnetic field components in the direction of motion bias the location of $B_{\max, \text{drape}}$ (figure to the right): draping is absent if $\mathbf{B} \parallel \mathbf{v}_{\text{gal}}$
- *geometric bias*: polarized synchrotron emission only sensitive to traverse magnetic field B_t (\perp to LOS) \rightarrow maximum polarised intensity may bias the location of $B_{\max, \text{drape}}$ towards the location in the drape with large B_t

